To appear in Journal of Experimental Mechanics

Models and control of fish-like locomotion

Juan Melli and Clarence W. Rowley

Department of Mechanical and Aerospace Engineering
Princeton University, Princeton, New Jersey

March 14, 2010

Abstract

Inspired by the advanced capabilities of fish-like swimmers, we seek a greater understanding of the hydrodynamic mechanisms they employ. Borrowing tools from geometric mechanics, we develop a large-amplitude gait design technique for self-propelling deformable swimmers in potential flow and Stokes flow. Additionally, a heuristically-developed control algorithm is implemented to nearly optimize thrust-generation for a swimmer moving through its own nearly-periodic vortex wake.

1 Motivation

The advanced capabilities of biological swimmers, including efficiency, maneuverability, and stealth, have attracted increased attention to the study of underwater swimming in recent years. For example, whereas sea lions have minimum turning radii of 9% of their body length [6], a traditional submarine's turning radius may be two to three body lengths or more [9]. An improved understanding of the hydrodynamic mechanisms and propulsion techniques employed by fish and other swimmers may lead to the design of more advanced man-made underwater vehicles.

Here we review the results from three simplified swimmer models used to study and better understand the locomotion of deformable bodies in a fluid. For the first two cases we consider articulated swimmers in both inviscid and highly viscous fluids. Although these two scenarios (modeled by potential flow and Stokes flow, respectively) are opposites in terms of the relative importance of inertial to frictional forces, they exhibit similar dynamical properties (they are both perfectly time-reversible systems) and

share a gait-design technique that we demonstrate. Finally, we consider a simplified model of a fish—tandem pitching and heaving hydrofoils—in which the trailing foil interacts with the vortex wake shed from the leading foil, and we present a heuristically-developed control technique to optimize the swimmer's thrust at steady-state.

2 Inviscid and highly viscous swimming

Although perhaps counter-intuitive, swimming—or more precisely, net translation and rotation due to cyclic internal shape changes—is in fact possible in a friction-free fluid even in the absence of vorticity or the exchange of momentum between the body and fluid. This net motion is known as geometric phase or holonomy. It is the same mechanism that allows a falling cat to rotate and land on its feet with no external torques, and therefore with zero angular momentum.

Another curious aspect of motion in an inviscid fluid is the notion of reversibility. That is, if a swimmer with only one joint were to move its tail back and forth, it would perfectly reverse its motion as the tail flaps in the opposite direction, and the swimmer would be unable to achieve net locomotion. Interestingly, this effect occurs in the opposite extreme of highly viscous flows as well. The "Scallop theorem" specifies that non-reciprocal motion is needed to swim in Stokes flow. Thus the simplest swimmer capable of achieving net motion in both inviscid, vorticity-free flows as well as in highly viscous flows is a two-hinged, three-link animal conceived by Purcell [14]. Much recent work has focused on this Purcell swimmer [3, 4, 15].

In the cases of both potential and Stokes flow swimmers, the equations of motion may be expressed in the following general form:

$$g^{-1}\dot{g} = -\mathcal{A}(\theta)\dot{\theta}. \tag{1}$$

In the case of the three-link Purcell swimmer, $g = (x, y, \beta)$ describes the overall planar position and orientation of the swimmer, while $\theta = (\theta_1, \theta_2)$ are the angles of its two joints, the *shape variables*. Hence, $\dot{g}$ is the velocity of the swimmer in an inertial reference frame, and $g^{-1}\dot{g}$ is the velocity in a frame fixed to the body (note that to define g^{-1}, we regard g as an element of the Lie group SE(2), and $g^{-1}\dot{g}$ is then an element of the Lie algebra $\mathfrak{se}(2)$). The term $\mathcal{A}(\theta)$ is a mathematical object called a *connection*, which relates internal shape change velocities, $\dot{\theta}$, to the overall velocity of the swimmer, $g^{-1}\dot{g}$. For instance, if $\dot{\theta} = (\dot{\theta}_1, \dot{\theta}_2)$ denotes the motion of the joint angles, and $g^{-1}\dot{g} = (\omega, u, v)$ denotes the overall velocity of the swimmer (in the

body-fixed frame), then the connection $\mathcal{A}(\theta)$ is a 3×2 matrix relating the two. The connection can be computed numerically for arbitrarily-shaped bodies via well-known boundary element panel methods. See [11] for details on the code and computing the connection for both potential and Stokes flow swimmers.

Equation (1) arises in a general theory of locomotion, in which the body's position and orientation g is an element of a Lie group, and the connection $\mathcal{A}$ is a Lie-algebra-valued one-form on the shape space. In the general theory, the connection $\mathcal{A}$ has the same general interpretation we use here, namely relating shape changes to motion in the group. For a thorough discussion of this formalism, see, for instance, [8, 7].

Studying the small-amplitude motion of deformable swimmers, Mason and Burdick [10] observed that the curvature, which is a type of derivative of the connection, "is an excellent measure of the effectiveness of the swimmer." In certain cases (namely, when the group is Abelian, or commutative), the process of designing large-amplitude gaits for such swimmers can be facilitated by visualizing the curvature of the connection, which can be computed numerically, over a grid on the shape space.

To understand how this works, note that a *gait* can be described by a closed curve in the shape space. As long as the group is Abelian (i.e., commutative, such as translations in one dimension), then the net translation over one cycle can be determined from the graph of the curvature of the connection. In particular, using Stokes' theorem, one can show that the net translation is the volume under this graph, enclosed by the closed curve corresponding to the gait. Thus, paths in shape space enclosing regions of high curvature correspond to more effective gaits. The process of designing gaits for both potential and Stokes flow swimmers thus becomes one of identifying regions of shape space corresponding to a desired volume of curvature.

This procedure works only for Abelian (commutative) groups, and many groups of interest, such as translations and rotations in two dimensions, are not Abelian. However, in [12] it was shown that this same procedure can be used at least for rotations in two dimensions, as the rotational component forms an Abelian component of the overall group (which can be described using a semidirect product structure).

As an example, in order to investigate turning motions of the swimmer, we may consider the rotation component of the connection $\mathcal{A}(\theta)$ (i.e., the first row of the matrix representation of $\mathcal{A}$), which we denote $\mathcal{A}_\omega(\theta) =$

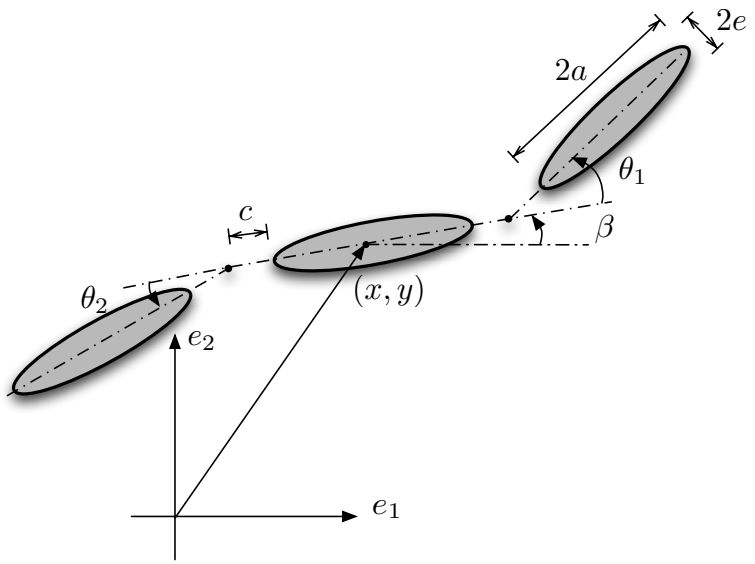

Figure 1: Schematic of 3-link articulated potential flow swimmer.

$(A_1(\theta), A_2(\theta))$. The rotation component of the curvature of $\mathcal{A}$ is then

$$F_\omega = \frac{\partial A_2}{\partial \theta_1} - \frac{\partial A_1}{\partial \theta_2}.$$

(Note that, for non-Abelian components, this formula includes an additional term arising from a Lie bracket—see [11] for details.)

Figure 2 shows the rotation component of the curvature F_ω for the potential flow swimmer shown in Figure 1 (where $a = 10, e = 1, c = 2$). This curvature component is largest in magnitude in two areas of shape space along $\theta_1 = -\theta_2$. These areas correspond to closed paths in shape space (gaits) which produce "effective" turning motions. One such path, chosen to enclose a curvature volume of $-\frac{\pi}{4}$, is indicated by the black circle. The result of the swimmer performing a gait specified by this circular path in shape space, beginning and ending at the dot on the circle, is shown in Figure 3. After completing the gait, the swimmer returns to its original shape, but has rotated clockwise by $\frac{\pi}{4}$ radians.

The same procedure can be used to develop gaits for the Stokes flow swimmer. We caution that in the case of planar motion, this large-amplitude gait design technique only applies for turning gaits and not forward or lateral gaits, because of the non-commutative nature of motion in the plane, as mentioned earlier. For further details on the gait design procedure, an

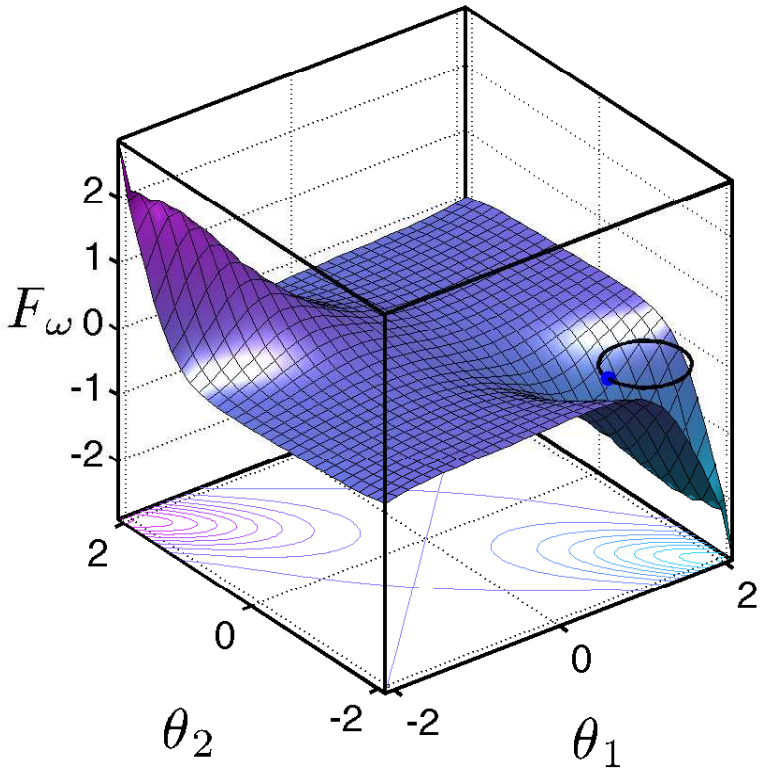

Figure 2: Rotation component of the curvature of the connection for a swimmer in potential flow. The circle specifies a path in shape space resulting in net rotation of $\frac{\pi}{4}$ radians. The path equation is given by $\theta_1(t) = 1.5 - .45\cos(t)$; $\theta_2(t) = -1.5 - .45\sin(t)$. The dot indicates the starting and end point of the particular gait.

explanation of when the large-amplitude design method applies, and how to use the curvature plots to design small-amplitude gaits in all directions, refer to [11].

3 Swimming through a vortex wake

Most practical swimmers operate somewhere between the extremes of potential and Stokes flow, relying on both viscous and inertial effects for locomotion. Thus we consider an extension of the potential flow model that partially accounts for the effects of viscosity through the shedding of vortic-

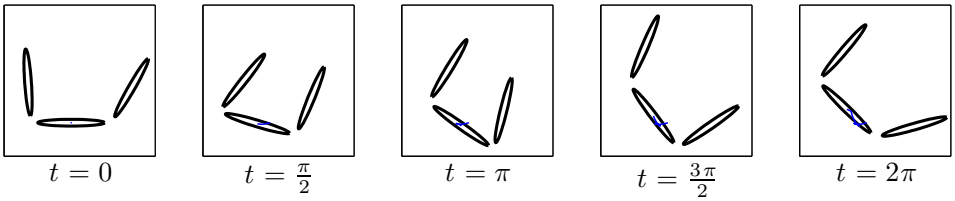

Figure 3: Snapshots of potential flow swimmer configuration during turning gait shown in Figure 2. The swimmer rotates by $\frac{\pi}{4}$ radians and returns to the original shape after one complete gait.

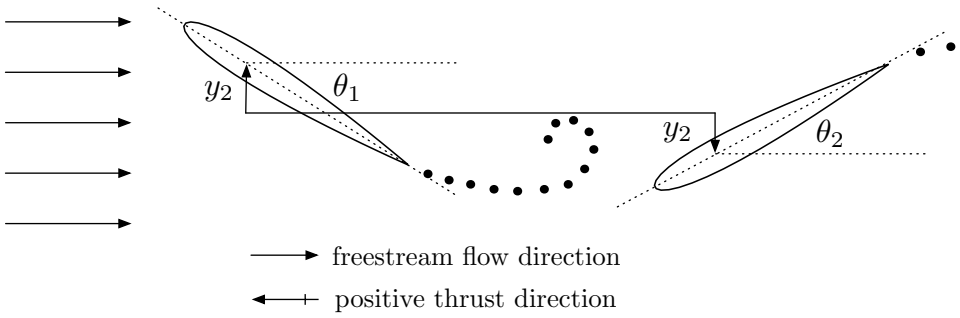

Figure 4: Schematic of tandem hydrofoil swimmer.

ity from a fin's trailing edge (the Kutta condition). In particular, we consider a swimmer composed of two hydrofoils, one leading the other, as shown in Figure 4. To compute the motion of this swimmer, we use a numerical model based on well-known panel methods [2, 13].

We are particularly interested in the interaction of the trailing foil with the nearly-periodic vortex wake shed from the leading foil. Others have hypothesized [5] based on experimental observations and later confirmed numerically [1] that the presence of upstream fins in fish can enhance thrust and efficiency. By adopting a heuristic approach and performing a series of numerical experiments, we have identified a mechanism responsible for enhancing thrust production.

During these numerical experiments, we varied the frequency of pitching and heaving (ω), the maximum pitching amplitude (A) and the phase difference between the leading and trailing foil, and we computed the average total thrust coefficient at steady state for each case. NACA 0012 hydrofoils were used, spaced 2.5 chord lengths apart, and pitched about the quarter

chord. We also monitored two additional quantities on the trailing foil as a function of time: the effective angle of attack due to only the motion of the foil while ignoring the influence of the effect of the wake (α_{eff}), and the position of the stagnation point on the leading edge (x_{stag}).

On physical grounds, it is plausible that the overall thrust could be related to the relationship between these two measured quantities: since x_{stag} captures the influence of the wake from the first foil, while α_{eff} is determined solely by the kinematics of the second foil, one might expect that maximum thrust would occur for a particular phase difference between these quantities, for which the wake interacts in a constructive manner. Figure 5 confirms this notion, and demonstrates that for the range of parameters considered in this study (namely, smaller-amplitude motions and lower frequencies), the steady-state thrust is nearly maximized when the phase difference between the two observed quantities ($\phi_D = \text{phase}(\alpha_{\text{eff}}) - \text{phase}(x_{\text{stag}})$) is zero. Note that here the foils are freely swimming, so the net thrust is zero. In Figure 5, we therefore consider the average thrust $\bar{T}$ needed to balance a simple model of skin friction drag (proportional to the square of the swimmer's velocity), and the nondimensional thrust coefficient is defined by $C_T = \bar{T}/(\rho(c/t_\omega)^2/2)$, where c is the chord, and t_ω is the period of pitching/heaving. Similar results to those shown in Figure 5 are also obtained when the velocity of the hydrofoils is prescribed (not freely swimming), for which the definition of thrust is more straightforward.

This result inspired a control strategy to optimize the thrust-production of the swimmer. The objective of this strategy is to ensure that the two quantities (α_{eff} and x_{stag}) on the trailing foil are in phase, and this was achieved by implementing a phase-locked loop controller.

Phase-locked loop controllers are designed to generate a signal with the same frequency and a fixed phase relative to a reference signal. In this case, the reference signal is the measured position of the stagnation point on the leading edge of the trailing foil. The controller then specifies a frequency for the pitching and heaving of the same foil such that the effective angle of attack of the trailing foil, α_{eff}, is phase-synchronized with the stagnation point position, x_{stag}.

In an example used to demonstrate the effectiveness of the controller, the leading foil is initially prescribed a fixed frequency of $\omega_1 = 7$. In the uncontrolled "baseline" case, the trailing foil is prescribed this same frequency, and a phase difference relative to the leading foil is chosen such that the steady-state thrust is optimized. Then, the frequency of the leading foil is varied as a function of time as shown in Figure 6, while that of the trailing foil remains constant—sometimes greater or less than the leading

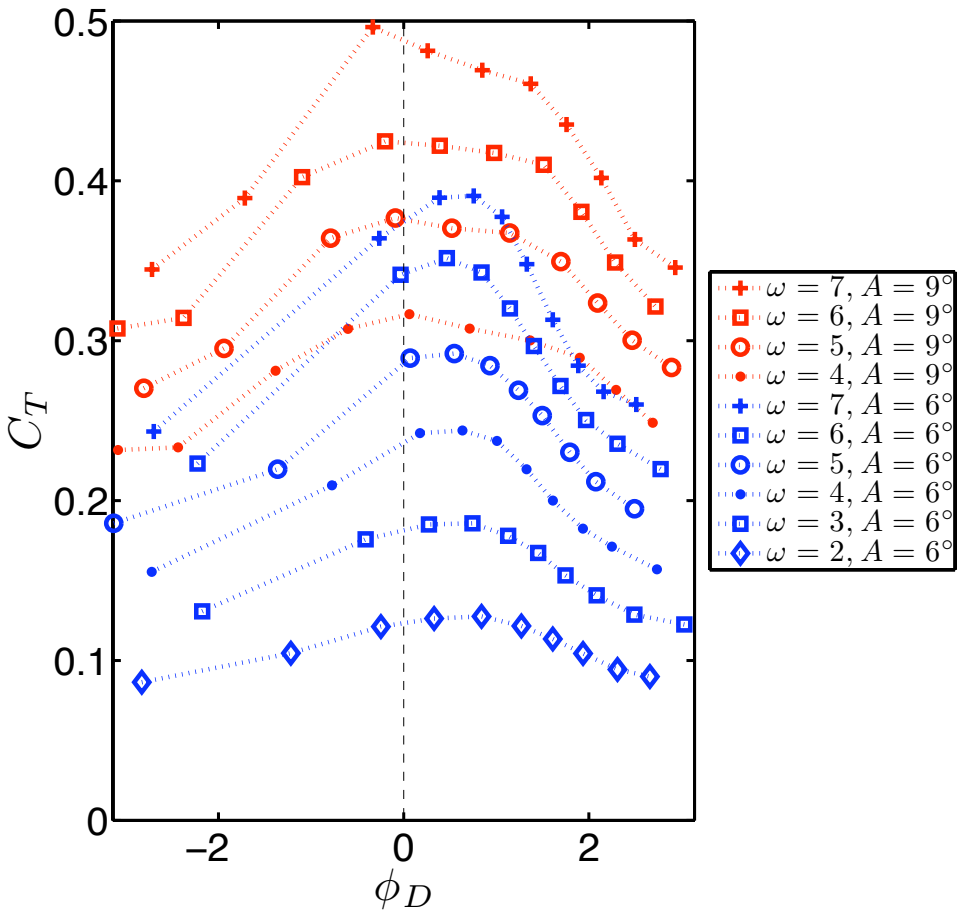

Figure 5: Average steady-state thrust coefficient (C_T) versus the phase difference between α_{eff} and x_{stag} at steady state for a series of numerical experiments.

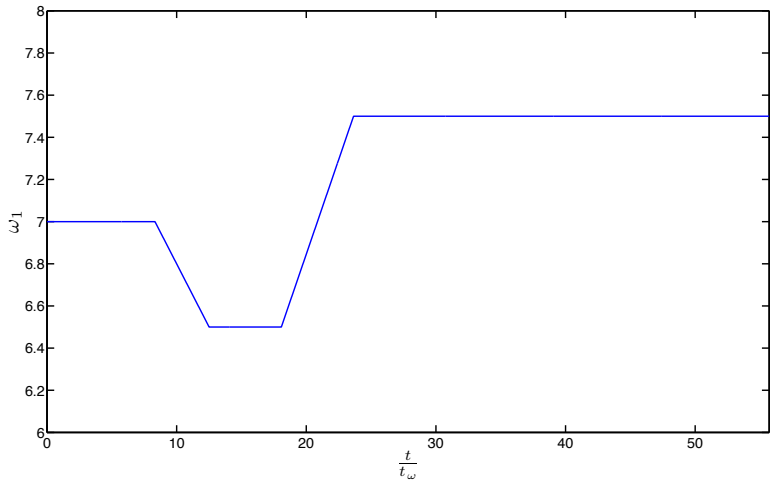

Figure 6: Leading foil frequency, $\omega_1(t)$ vs non-dimensionalized time. The frequency of the leading foil is varied from its initial value in order to evaluate the effectiveness of applying control to the trailing foil.

foil's frequency. On the other hand, a second case uses the phase-locked loop controller to adapt to the changing wake frequency due to the variable leading foil frequency.

Figure 7 demonstrates the effectiveness of the controller by comparing the velocity of the swimmer during both controlled and uncontrolled cases. A snapshot of the swimmer and wake for the controlled case is shown in Figure 8. Even when the controller slowed the trailing foil frequency as a result of the reduced leading foil frequency, the swimmer using the controller propelled faster than in the uncontrolled case. Further, for this example, the controller resulted in a higher swimmer speed, decreased power use and higher propulsive efficiency.

4 Conclusions

The morphological and physiological diversity of fish-like swimmers implies a rich variety of hydrodynamic forms of propulsion. Here we have presented three models in order to understand a subset of those hydrodynamic mechanisms, and design gaits for efficient motion of fish-like underwater vehicles.

For potential flow and viscous flows, a mathematical object called the connection can be used to design gaits to achieve a desired net angle of rotation. For a more complex model including vortex shedding, we have studied

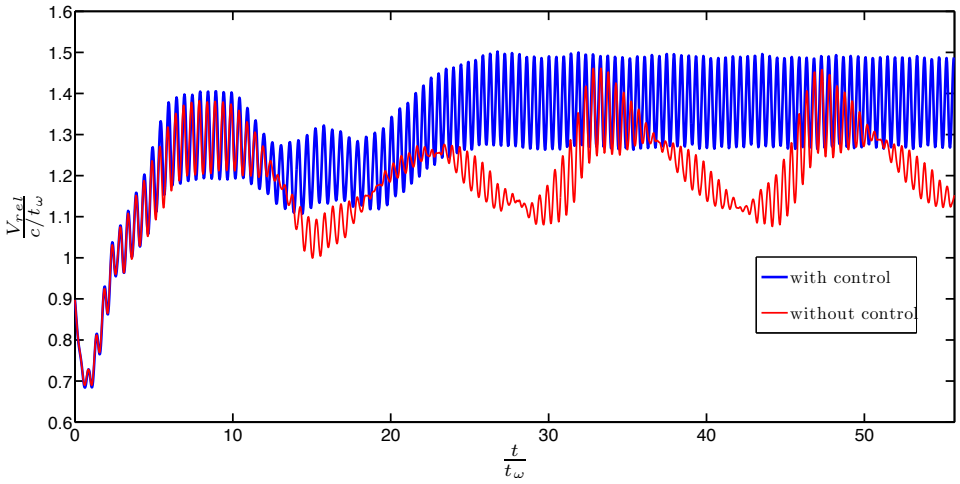

Figure 7: Comparison of relative speed vs non-dimensionalized time for a swimmer with (blue) and without (red) control. A snapshot of the swimmer and flow field for the controlled case is shown in Figure 8.

a specific geometry consisting of two hydrofoils (designed to conceptually represent dorsal and caudal fins), and we have presented a feedback control law that adjusts the phase of the trailing foil to improve thrust production, based on the location of the instantaneous stagnation point near the leading edge of the trailing fin. For further details on these models and additional references on the modeling and control of fish-like locomotion, we refer the interested reader to [11, 12].

References

[1] Akhtar, I., Mittal, R., Lauder, G., and Drucker, E. Hydrodynamics of a biologically inspired tandem flapping foil configuration. *Theoretical and Computational Fluid Dynamics 21*, 3 (2007), 155–170.

[2] Basu, B., and Hancock, G. The unsteady motion of a two-dimensional aerofoil in incompressible inviscid flow. *J. Fluid Mech. 87*, 1 (1978), 159–178.

[3] Becker, L., Koehler, S., and Stone, H. On self-propulsion of micro-machines at low Reynolds number: Purcell's three-link swimmer. *Journal of Fluid Mechanics 490* (2003), 15–35.

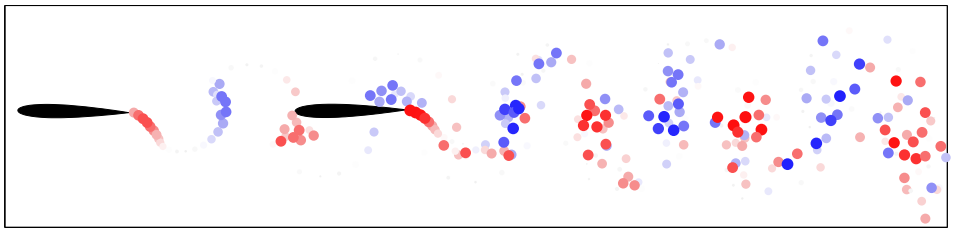

Figure 8: Snapshot of swimmer and vortex wake. A portion of the wake of the swimmer is shown for the controlled case at $t/t_\omega = 44.5$. The red and blue circles represent clockwise and counterclockwise vorticity, respectively. The larger, darker circles correspond to stronger strength vortices while the smaller, lighter circles are weaker strength vortices.

[4] de Araujo, G., and Koiller, J. Self-Propulsion of N-Hinged 'Animats' at Low Reynolds Number. *Qualitative Theory of Dynamical Systems 1* (2003), 1–28.

[5] Drucker, E. G., and Lauder, G. V. Locomotor function of the dorsal fin in teleost fishes: experimental analysis of wake forces in sunfish. *J. Exp. Biol. 204* (2001), 2943–2958.

[6] Fish, F. Performance constraints on the maneuverability of flexible and rigid biological systems. *Proceedings of the Eleventh International Symposium on Unmanned Untethered Submersible Technology* (1999), 394–406.

[7] Kanso, E., Marsden, J. E., Rowley, C. W., and Melli-Huber, J. B. Locomotion of articulated bodies in a perfect fluid. *J. Nonlin. Sci.* (2005).

[8] Kelly, S. D. *The Mechanics and Control of Robotic Locomotion with Applications to Aquatic Vehicles*. PhD thesis, California Institute of Technology, Pasadena, California, May 1998.

[9] Maslov, N. Maneuverability and controllability of dolphins. *Bionika 4* (1970), 46–50.

[10] Mason, R., and Burdick, J. W. Propulsion and control of deformable bodies in an ideal fluid. In *IEEE International Conference on Robotics and Automation* (1999).

[11] Melli, J. B. *A hierarchy of models for the control of fish-like locomotion*. PhD thesis, Princeton University, Princeton, NJ, September 2008.

[12] Melli, J. B., Rowley, C. W., and Rufat, D. S. Motion planning for an articulated body in a perfect planar fluid. *SIAM J. Appl. Dyn. Sys. 5*, 4 (2006), 650–669.

[13] Pang, C.-K. A Computer Code (USPOTF2) for Unsteady Incompressible Flow Past Two Airfoils. Master's thesis, Naval Postgraduate School, Monterey, California, September 1988.

[14] Purcell, E. M. Life at low Reynolds number. *Am. J. Phys. 45*, 1 (Jan. 1977), 3–11.

[15] Tam, D., and Hosoi, A. Optimal Stroke Patterns for Purcell's Three-Link Swimmer. *Physical Review Letters 98*, 6 (2007), 68105.